Journal of General Virology (2010), **91**, 643–652 DOI 10.1099/vir.0.016063-0

Production, characterization and *in vitro* testing of HBcAg-specific VHH intrabodies

Benedikte Serruys, Freya Van Houtte, Ali Farhoudi-Moghadam, Geert Leroux-Roels and Peter Vanlandschoot

Center for Vaccinology, Ghent University and Hospital, Ghent, Belgium

Correspondence
Geert Leroux-Roels
geert.lerouxroels@ugent.be

Received 26 August 2009
Accepted 4 November 2009

Hepatitis B virus (HBV) infections represent a global health problem, since these account for 350 million chronic infections worldwide that result in 500 000–700 000 deaths each year. Control of viral replication and HBV-related disease and mortality are of utmost importance. Because the currently available antiviral therapies all have major limitations, new strategies to treat chronic HBV infection are eagerly awaited. Six single-domain antibodies (VHHs) targeting the core antigen of HBV (HBcAg) have been generated and three of these bound strongly to HBcAg of both subtype *ayw* and *adw*. These three VHHs were studied as intrabodies directed towards the nucleus or the cytoplasm of a hepatoma cell line that was co-transfected with HBV. A speckled staining of HBcAg was observed in the cytoplasm of cells transfected with nucleotropic VHH intrabodies. Moreover, an increased intracellular accumulation of hepatitis B e antigen (HBeAg) and a complete disappearance of intracellular HBcAg signal were observed with nuclear targeted HBcAg-specific VHHs. These results suggest that HBcAg-specific VHHs targeted to the nucleus affect HBcAg and HBeAg expression and trafficking in HBV-transfected hepatocytes.

INTRODUCTION

Control of the replication cycle of hepatitis B virus (HBV) is of vital importance since there are still 2 billion people worldwide infected with HBV and 350 million suffering from a chronic infection. Approximately 15–40 % of these chronically infected people will develop cirrhosis, liver failure and hepatocellular carcinoma (HCC), leading to 500 000–700 000 deaths each year (Lavanchy, 2004). Therapies with interferons (IFNs) and nucleos(t)ide analogues are the only approved treatments for chronic HBV infections, but these all have serious drawbacks (Hilleman, 2003; Seeger *et al.*, 2007).

Novel approaches are currently being explored to tackle HBV infection. The hepatitis B core antigen (HBcAg) is an attractive target for new therapeutic candidates. This molecule is the structural unit of the nucleocapsid, which surrounds the partially double-stranded viral DNA genome within the viral particle. Nucleocapsids are formed of 180 or 240 HBcAg monomers in the cytoplasm, encapsidating one copy of viral pre-genomic RNA (pgRNA) (Bruss, 2004, 2007). After conversion of the pgRNA into a mature viral genome, the nucleocapsid moves to the endoplasmic reticulum (ER) where it interacts with the ER membrane-embedded viral envelope proteins. This results in the construction of a complete viral particle, which is transported further in the secretory pathway. Finally, the particles are secreted into the bloodstream. The cytoplasmic mature nucleocapsids can also move back to the nucleus, disintegrate into individual HBcAg molecules in the nuclear pore complex and finally release the viral genome into the nucleus (Kann *et al.*, 2007; Rabe *et al.*, 2003). The number of nuclear viral genomes is amplified by this recycling mechanism (Tuttleman *et al.*, 1986). HBcAg proteins in the nucleus function as transcriptional inhibitors of the IFN-induced antiviral MxA protein (Gordien *et al.*, 2001; Rosmorduc *et al.*, 1999). These individual HBcAg molecules in the nucleus can again reassemble into nucleocapsids. The biological role of this nuclear capsid remains unresolved. It has been shown, by several research groups, that the presence of capsid in the nucleus is correlated with a high level of viral replication and a low degree of hepatocyte proliferation (Kim *et al.*, 2006; Serinoz *et al.*, 2003).

Several core-specific small molecule antivirals have shown that HBcAg is indeed a good candidate for inhibition of HBV replication (Feld *et al.*, 2003; Xu *et al.*, 2003). These core-specific antivirals may act at either the RNA level or the protein level. Efficient viral inhibition by targeting the core RNA, which is in fact the pgRNA, has already been demonstrated with RNA interference (Ying *et al.*, 2003), antisense oligonucleotides (Ji & Si, 1997) and ribozymes (Feng *et al.*, 2001). HBcAg has also been targeted at the protein level by aptamers (Butz *et al.*, 2001),

Four supplementary figures and a supplementary table of primer sequences are available with the online version of this paper.

HeteroArylDihydropyrimidines or HAPs (Deres *et al.*, 2003) and single-chain variable fragment (scFv) intrabodies (Yamamoto *et al.*, 1999).

Recently, we have described the inhibitory potential of VHH intrabodies directed against the most abundant domain, S, of the envelope proteins of HBV. A more than two log reduction in virion secretion was observed in mice 11 days after the injection of a plasmid coding for an anti-S VHH intrabody (Serruys *et al.*, 2009). Based on the successful targeting by experimental small molecule drugs against HBcAg, we have explored whether VHH intrabodies against HBcAg are able to inhibit HBV replication. In this report, we describe the production and biochemical characterization of HBcAg-specific VHH molecules. We studied the expression of the corresponding VHH intrabodies in the cytoplasm as well as in the nucleus and tested these in a cellular HBV model.

RESULTS

Isolation and selection of HBcAg-specific VHHs

Two llamas were immunized with recombinant HBcAg (Diasorin, subtype *ayw*) to induce the production of HBcAg-specific antibodies. The VHH phage library was created as described previously (Serruys *et al.*, 2009). The VHH entities of the library were expressed on phages after infection of the bacteria with the helper phage M13K07. Selection of HBcAg-specific VHHs was performed by one round of biopanning. Ninety-four bacterial colonies were randomly chosen and induced for the secretion of soluble VHH molecules that were screened for target specificity by a VHH-screening ELISA. Eighty per cent of all VHH–p3 fusion proteins bound their antigen. The presence of VHH-coding phagemids in the bacteria was confirmed by colony PCR. *Hin*fI fingerprinting showed 34 VHH-coding genes with a different restriction pattern. These were sequenced, aligned and subdivided into 21 families. Finally, six HBcAg-specific VHHs were selected (C1–C6) based on their sequence (Fig. 1) and on their antigen-binding capacity (Table 1). As a negative control, VHH NC, a VHH molecule that does not bind HBcAg, was used (Serruys *et al.*, 2009).

Characterization of HBcAg-specific VHH molecules

Binding of the VHH molecules to HBcAg was studied by a VHH-binding ELISA using HBcAg, taken from two HBV strains, one with HBcAg subtype *ayw* and the other with HBcAg subtype *adw*. The non-HBcAg-specific VHH NC and a monoclonal mouse anti-HBcAg antibody were included as negative and positive controls, respectively. Based on the obtained optical density, the VHHs were divided into two groups (Fig. 2a). The first group consisted

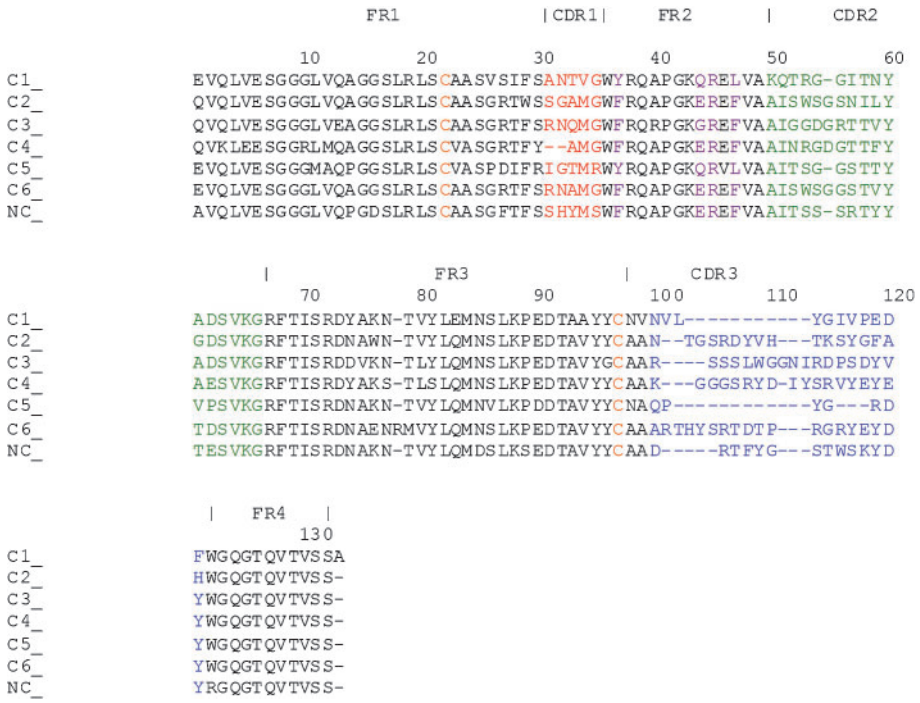

Fig. 1. Amino acid sequences of the six selected HBcAg-specific VHHs (C1–C6) and the non-HBcAg-specific VHH (NC). The framework regions (FR) and complementary determining regions (CDR) are indicated. CDR1 is highlighted in red, CDR2 in green and CDR3 in blue. Residues in purple represent residues that are characteristic for camelids. Residues in orange represent cysteines that can form disulphide bridges.

Table 1. A_{405} in the VHH-screening ELISA of the six selected HBcAg-specific VHHs (C1–C6)

Clone	A_{405}
C1	0.175
C2	1.100
C3	0.325
C4	1.332
C5	0.248
C6	0.854
Background	0.081

of VHHs C2, C4 and C6 which bound very well to both *ayw* and *adw* HBcAg and also elicited the best signal in the VHH-screening ELISA (Table 1). VHHs C2 and C4 bound to HBcAg at the same level as the positive control mouse anti-HBc. Taking into account that these VHHs are monovalent while the monoclonal antibody (mAb) is a bivalent molecule, these results indicated that the VHHs probably have a high affinity for their antigen. The second group consisted of VHHs C1, C3 and C5 which induced a lower signal in the VHH-binding ELISA, with a very weak binding of C3 and no binding of C5 to subtype *adw*.

The sequences of both HBcAg preparations are described in Supplementary Fig. S1 (available in JGV Online). The major sequence differences are situated within or surrounding the immunodominant tip of HBcAg. The difference in binding signal of VHHs C3 and C5 to the two HBcAg molecules suggests that this tip may be part of the epitope. The importance of this region for C3 and C5 has also been demonstrated by the loss in binding to an *ayw* HBcAg mutant with a deletion within the tip (Supplementary Fig. S2). The binding of C2, C4 and C6 to this deletion mutant was also abolished, suggesting that the tip is also important for these VHHs although differences in the amino acid composition in the tip with *adw* HBcAg did not seem to affect the binding. In contrast, VHH C1 bound equally well to the wild-type HBcAg *ayw* as to its deletion mutant, suggesting that the epitope of C1 is not located in the tip. Indeed, although C1 has no high binding capacity for HBcAg, it bound to both HBcAg *ayw* and *adw*.

The anti-HBcAg activity of the VHHs was studied further by a routine qualitative competition assay for anti-HBcAg detection (AxSYM CORE, Abbott). According to the manufacturer's guidelines, serum samples with a signal-to-cutoff (S/Co) ratio of less than 1.0 were considered positive for anti-HBcAg antibodies. VHHs C2 and C4 gave a positive result with ± 70 nM (approximately 1 μg ml^{-1}) (Fig. 2b), suggesting that they did interfere with the binding of the detection antibodies of the commercial test kit. The other VHHs were negative in the competition assay.

HBcAg and hepatitis B e antigen (HBeAg) are both translated from the pgRNA, initiating from different start codons within the same open reading frame. Therefore, HBcAg and HBeAg share a large part of their amino acid sequence. In contrast with HBcAg, HBeAg is produced in a non-particulate form and is secreted into the bloodstream as dimers. Despite their differences in conformation and coding sequence, HBcAg and HBeAg share antigenic epitopes. Therefore, we checked if the VHHs were cross-reactive for HBeAg. VHHs C4 and C6 indeed bound HBeAg (Fig. 2c), while the other VHHs did not show any cross-reactivity.

Based on the results of the VHH-binding ELISA, only the strong binders C2, C4 and C6 were investigated in more detail.

Cloning the VHH coding sequence in a eukaryotic vector

HBcAg exerts its functions in different compartments of the infected cell. Cytoplasmic localization is required for the formation of the nucleocapsid first and of complete viral particles thereafter (Bruss, 2004, 2007), while nuclear localization of HBcAg is required to fulfil the role of IFN inhibitor (Gordien *et al.*, 2001; Rosmorduc *et al.*, 1999) and is thought to be associated with high-level replication (Kim *et al.*, 2006; Serinoz *et al.*, 2003). To interfere with these different functions of HBcAg, expression of HBcAg-specific VHHs as intrabodies was targeted to the cytoplasm as well as to the nucleus. For this, the VHH coding sequence and the adjoining His-tag were cloned into the cytoplasmic plasmid pCMV/*myc*/cyto and in the nuclear plasmid pCMV/*myc*/nuc (pShooter; both Invitrogen), using the *Nco*I and *Not*I restriction sites. The nuclear vector contains a triple nuclear localization signal from the SV40 large T antigen. Because the coding sequence of VHHs C2, C4 and C6 contains an internal *Nco*I restriction site, a nucleotide substitution without any change in the amino acid composition was performed prior to the construction of the corresponding pShooter vectors.

Effect of the VHHs in a cellular HBV model

We previously used the HBV coding plasmid pSP65*ayw*1.3 (a kind gift from Frank Chisari, The Scripps Research Insitute) which encodes HBcAg subtype *ayw* (GenBank accession no. V01460) (Serruys *et al.*, 2009). To examine the effect of the VHHs on HBcAg of subtype *adw* as well as *ayw*, another pSP65 plasmid coding for HBcAg of subtype *adw* (GenBank accession no. 51970) (produced by GeneArt, Regensburg) was constructed. This new vector was called pSP65*adw*1.3. To compare the production of viral proteins of both plasmids, a series of electroporations were performed and the levels of secreted hepatitis B surface antigen (HBsAg) and HBeAg, and the amounts of intracellular HBcAg were determined. All data were comparable for both HBV plasmids (Fig. 3a), implying that the introduction of *adw* HBcAg to the plasmid did not negatively affect the production of viral proteins. Both

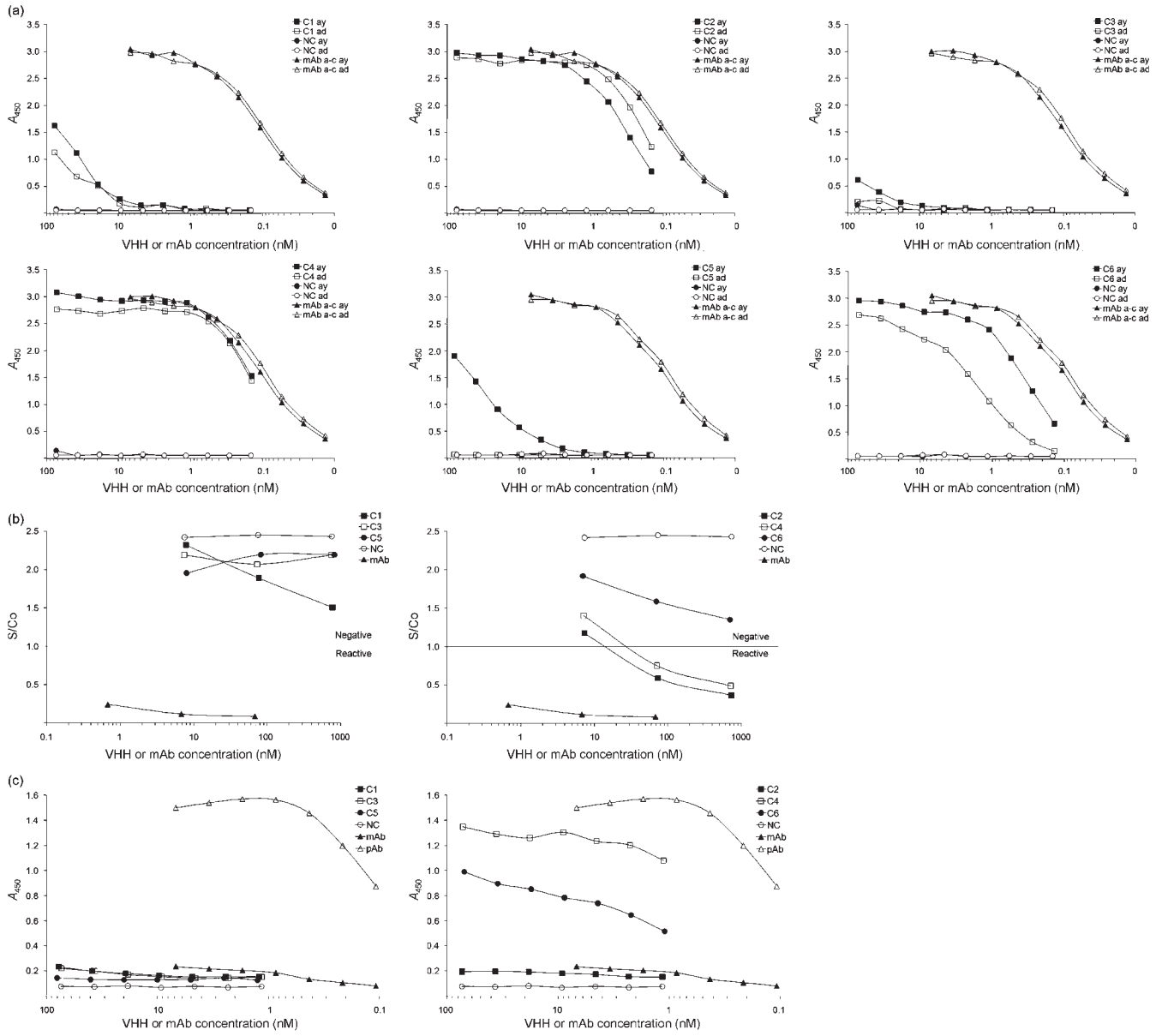

Fig. 2. Binding characteristics of the HBcAg-specific VHHs (C1–C6), the non-HBcAg-specific VHH NC as negative control and a monoclonal mouse anti-HBcAg antibody as a positive control. (a) Study of the binding of the *E. coli*-purified VHH molecules on HBcAg subtypes *ayw* and *adw* by a VHH-binding ELISA. (b) Detection of anti-HBcAg activity by AxSYM CORE. (c) Binding of the VHH molecules on 1 μg ml^{-1} coated HBeAg. A monoclonal (mAb) and a polyclonal (pAb) anti-core antibody were included as control antibodies.

plasmids are consequently equivalent for the study of VHH activity.

Before the antiviral capacity of the VHHs was investigated, a sandwich-VHH-binding ELISA was performed to investigate if the VHHs recognized expressed HBcAg of cells transfected with 10 μg HBV plasmid. Therefore, 45 μg total lysate was added to a rabbit anti-core coated Maxisorp plate. Binding of *Escherichia coli*-purified VHH with HBcAg lysate was compared to binding with commercially available recombinant HBcAg preparations. All three VHH molecules recognized *ayw* HBcAg as well as *adw* HBcAg in the lysates (Fig. 3b), thus confirming that VHHs recognize nucleocapsids produced by HBV plasmid-transfected hepatoma cells in addition to recombinant nucleocapsid.

The optimal harvesting time point and concentration of transfected HBV plasmid needed to obtain the highest yield of HBcAg was determined before the effect of co-expression of VHH intrabodies was investigated. For this, the hepatoma cell line HepG2 was transfected with

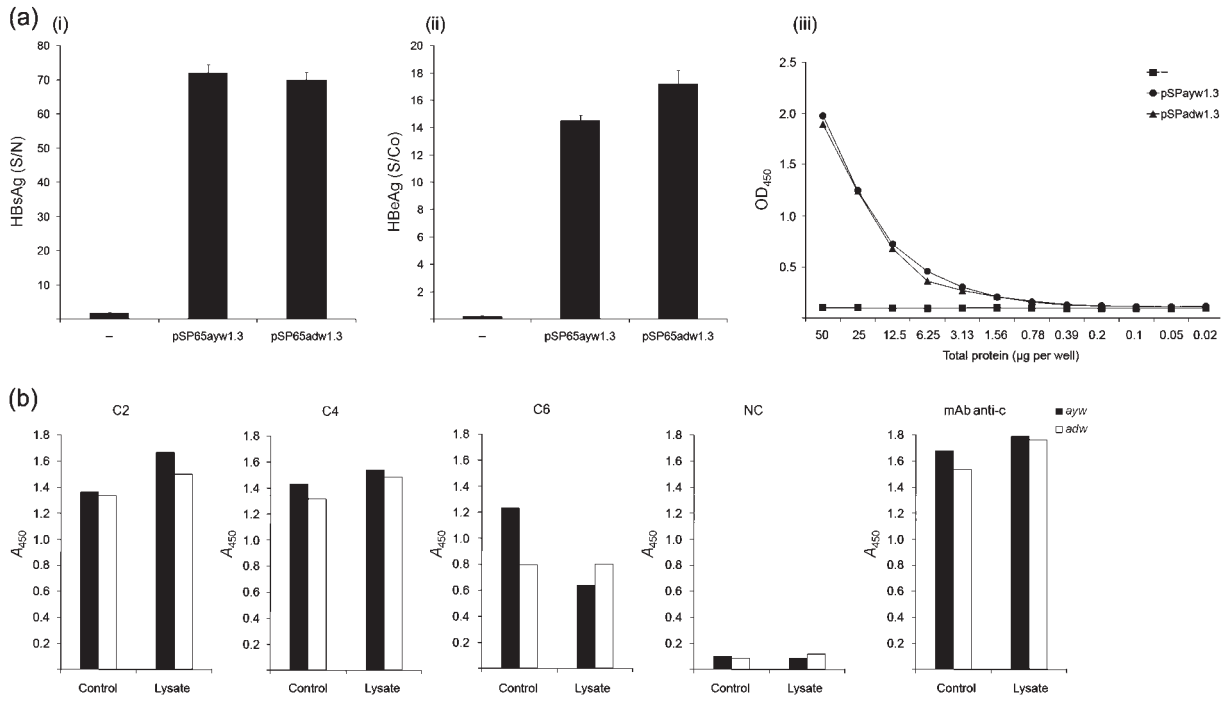

Fig. 3. (a) Comparison of cells transfected with 10 µg *ayw* or *adw* HBV plasmid for the secretion of HBsAg (i) and HBeAg (ii) and the amount of intracellular HBcAg (iii). (b) A sandwich-VHH-binding ELISA was performed to study VHH binding to HBcAg present in 45 µg total lysate obtained following transfection of cells with 10 µg HBV plasmid. The binding of VHH to this material was compared with that of commercially available HBcAg (50 ng ml^{-1}; Control). Filled bars, *ayw*; open bars, *adw*.

various amounts of HBV plasmid (5, 10, 25 and 50 µg), complemented with stuffer empty pShooter plasmid, to obtain a total of 50 µg DNA. The cells were lysed at 1, 2 or 3 days post-electroporation. Transfection of 25 and 50 µg HBV plasmid did not result in a sufficient number of viable cells, suggesting that a high amount of HBV plasmid was toxic for the cells. Consequently, the HBcAg level was not determined for the transfections using 25 and 50 µg HBV plasmid. Transfections with 5 and 10 µg were not toxic and the highest quantity of HBcAg was measured at 3 days after transfection with 10 µg HBV DNA (Table 2). Therefore, further transfections to study the effect of VHH intrabodies on HBV were performed with 10 µg HBV plasmid. This was further complemented with 2 µg pShooter VHH plasmid and 8 µg empty pShooter vector, resulting in a total of 20 µg plasmid. Three days post-electroporation, supernatant was collected and lysates were prepared or cells were immunostained for confocal microscopy.

Confocal microscopy analysis showed that the VHHs were present in the targeted compartments: cytoplasm-directed VHH was localized in the cytoplasm and nucleus-targeted VHH was predominantly present in the nucleus (Fig. 4 and Supplementary Fig. S3). This indicates that the VHH molecules were efficiently expressed in the reducing environment of the cytoplasm and transported to the nucleus, despite the lack of disulphide bridges. The cells were also stained for HBcAg to examine whether the HBcAg-specific VHHs had any influence on the cellular distribution of HBcAg. No difference was observed in HBcAg distribution between the cytoplasm-directed VHHs and the negative control groups. All groups showed a diffuse cytoplasmic staining. In contrast, a more speckled distribution of HBcAg was noted in the cytoplasm with the HBcAg-specific VHHs directed to the nucleus, suggesting that nuclear VHHs affect HBcAg distribution.

Next, the levels of secreted and intracellular HBsAg and HBeAg were determined to see if the VHHs influenced the

Table 2. Determination of the optimal harvesting point and concentration of HBV plasmid needed to obtain the highest amount of HBcAg, by using an HBcAg-binding assay

Values represent the OD_{450}. NA, Not applicable.

HBV plasmid	Amount (µg)	Days post-transfection		
		1	2	3
Negative control	NA	0.101	0.098	0.097
Ay	5	0.107	0.160	0.206
	10	0.118	0.192	0.242
Ad	5	0.106	0.162	0.194
	10	0.154	0.341	0.312

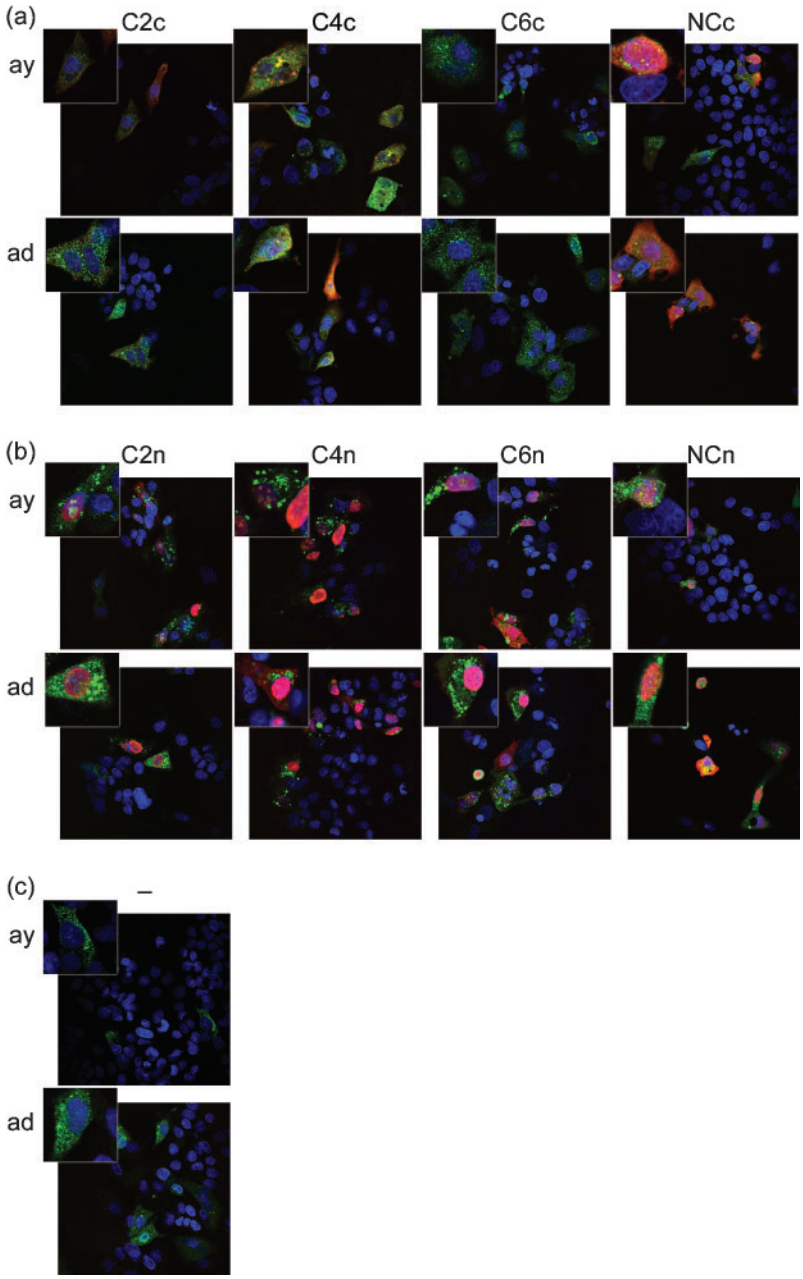

Fig. 4. Immunofluorescent staining of HBcAg (green), VHH (red) and nuclei (blue). HepG2 cells were transfected with 10 μg pSP*ayw*1.3 or pSP*adw*1.3 plasmid, 2 μg VHH–pShooter vector pCMV/*myc*/cyto (a) or pCMV/*myc*/nuc (b) and 8 μg empty pShooter plasmid (3 days post-electroporation). A negative control electroporation was performed without VHH–pShooter plasmid (c). Cotransfection with a nuclear-directed VHH shows a speckled HBcAg pattern. The complete staining experiment, including VHH and nuclei staining, is shown in Supplementary Fig. S3.

production and secretion of other viral proteins (Fig. 5). The amount of secreted HBsAg and HBeAg was comparable for all groups (Fig. 5a), as was the amount of intracellular HBsAg. In contrast, an increase in intracellular HBeAg was demonstrated when the VHHs C2 and C6 were localized in the nucleus (Fig. 5b). This elevation was predominantly observed with the *adw* HBV plasmid and was also demonstrated with 10 μg instead of 2 μg VHH plasmid (Supplementary Fig. S4). No difference in the amount of secreted viral particles was observed.

Finally, the amount of capsid in the lysates was determined using an HBcAg detection ELISA. The HBcAg signal dropped to background levels with all nuclear HBcAg-specific VHHs, while the non-HBcAg-specific VHH NC had no effect on the amount of HBcAg detected (Fig. 6). In summary, the elevated intracellular amount of HBeAg and the observed absence of HBcAg in lysates with VHHs targeted to the nucleus suggest that these specifically affect HBcAg and HBeAg pathways.

DISCUSSION

In this study, we describe the production and *in vitro* characterization of six VHH molecules directed against HBcAg. The binding affinity for HBcAg of three of these VHHs (C2, C4 and C6) was comparable with that of a

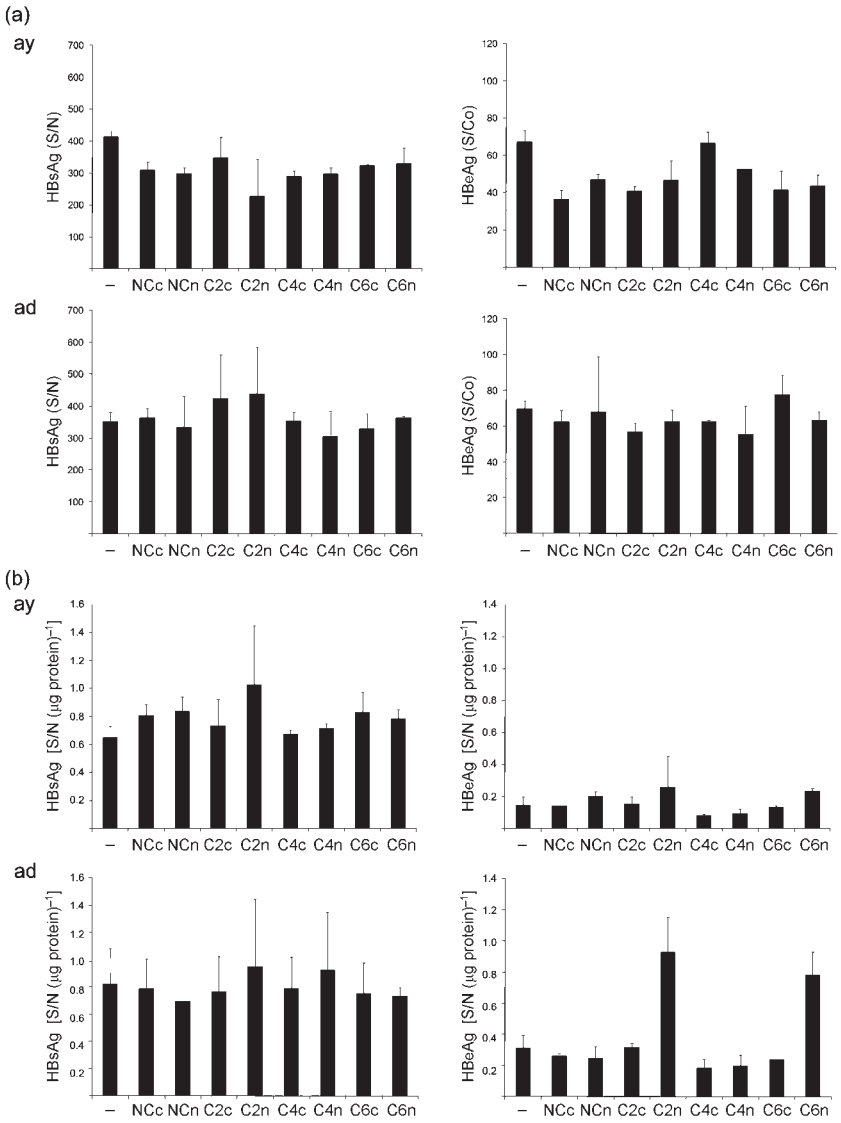

Fig. 5. Determination of HBsAg and HBeAg levels in cell culture medium (a) and cell lysate (b). HepG2 cells were transfected with 10 µg pSP*ayw*1.3 or pSP*adw*1.3 plasmid, 2 µg VHH–pShooter vector and 8 µg empty pShooter plasmid (3 days post-electroporation). S/N, Signal-to-noise; S/Co, signal-to-cutoff.

reference mAb (Fig. 2a). Taking into account that the VHHs are monovalent while the mAb is bivalent, these VHH molecules must have excellent antigen-binding properties. VHHs C4 and C6 also bind to HBeAg, suggesting that these bind an epitope shared by HBcAg and HBeAg. Furthermore, C2 and C4 gave a positive result in the AxSYM CORE test (Fig. 2b), indicating that these VHHs interfered with the binding of the antibodies present in the kit. The negative results of the other VHHs in the AxSYM CORE test may be due to: (i) the smaller size of the VHHs compared with the detection antibodies that bind the same epitope; (ii) the binding of these VHHs on a different epitope to the detection antibodies; or (iii) a lower affinity of the VHHs. The latter was already suggested by the lower OD signal in the VHH-screening ELISA and the VHH-binding ELISA, especially for C1, C3 and C5.

The three *E. coli*-derived VHH molecules that strongly interacted with recombinant HBcAg (C2, C4 and C6) were also capable of binding capsids derived from *ayw* as well as *adw* HBV-transfected HepG2 cells (Fig. 3b). This allowed the study of these VHHs as cytoplasmic and nuclear intrabodies in HBV-transfected cells and their possible effect on expression and assembly of HBcAg and/or other viral proteins.

The study of HBV-transfected cells showed an increase in intracellular HBeAg with nuclear VHH intrabodies C2 and C6, predominantly with *adw* HBV. This phenomenon may be caused by the interference of VHH intrabodies with the formation of complete capsid particles. These non-particulate HBcAg molecules may display HBeAg antigenicity, resulting in their detection as HBeAg in the automated test. Another hypothesis for the increase in intracellular HBeAg may be the recognition of HBeAg by C2 and C6, resulting in retention inside the cell. However, only C4 and C6 display cross-reactivity for HBeAg (Fig. 2c). Moreover, the unchanged secreted level of HBeAg does not support this view.

Confocal microscopy revealed a speckled staining of HBcAg in the cytoplasm with nuclear HBcAg-specific VHHs (Fig. 4).

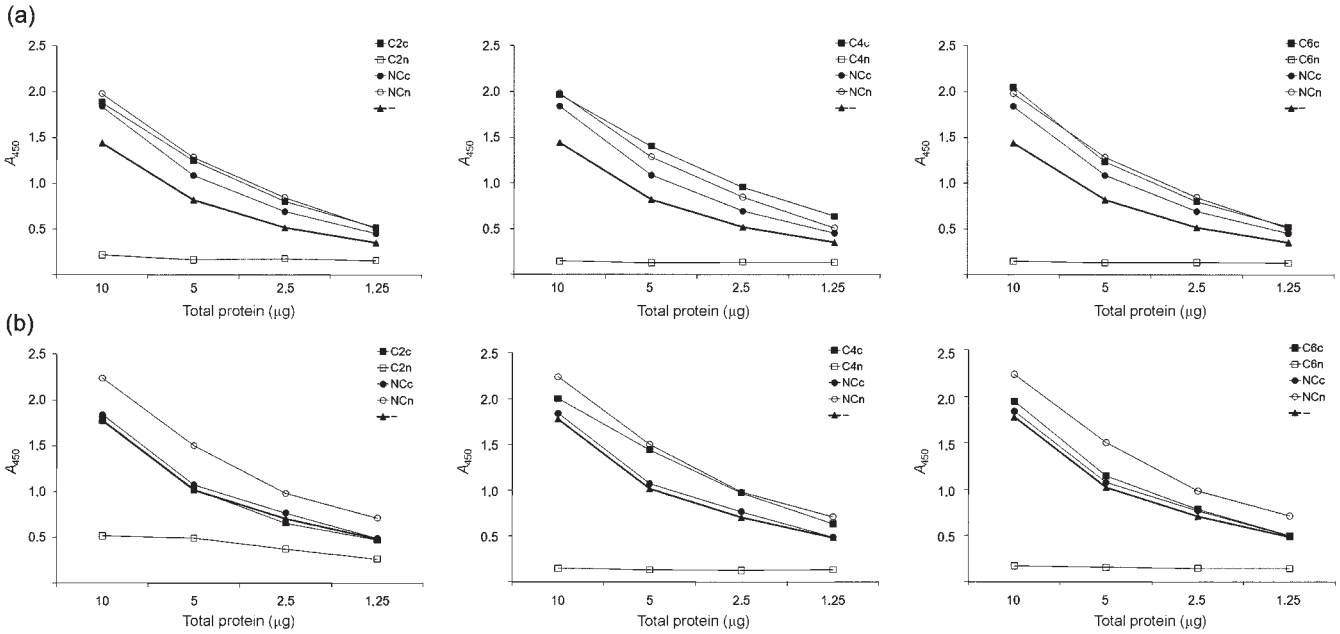

Fig. 6. Detection of intracellular HBcAg content in cells cotransfected with 10 μg pSP*ayw*1.3 (a) or pSP*adw*1.3 (b) plasmid, 2 μg VHH–pShooter vector and 8 μg empty pShooter plasmid (3 days post-electroporation). The presence of HBcAg in HBcAg-specific VHH-transfected cells was compared with transfections without VHH (–) or with the non-HBcAg-specific VHH NC.

It is possible that the VHHs targeted to the nucleus indirectly affect HBcAg in the cytoplasm, resulting in an accumulation of HBcAg. Another possible explanation is that this signal may be due to an accumulation of HBeAg instead of HBcAg. Indeed, the polyclonal antibody used to detect HBcAg also interacts with HBeAg (Fig. 2c). However, this result is not consistent with the increased level of intracellular HBeAg by AxSYM detection (Fig. 5b), since nuclear C4 also shows these cytoplasmic speckles while the intracellular level of HBeAg was not increased with nuclear C4.

In contrast with the results obtained using confocal microscopy, only background levels of HBcAg in lysates were observed with all nuclear VHHs (Fig. 6). No clear explanation is available for the absence of this HBcAg signal in the ELISA. Inhibition of HBcAg binding on the coated anti-HBcAg antibody by VHH is unlikely because the HBcAg level with co-expressed cytoplasmic VHH did not give a background signal. Moreover, we have checked whether an inhibition may occur by co-incubating HBcAg with HBcAg-specific VHHs on an anti-HBcAg coated plate. A limited inhibition of the signal was observed when a very high concentration of VHH was applied (data not shown). It is very unlikely that this interference is responsible for the low levels of HBcAg in the lysates, since these contained only small amounts of VHHs.

To our knowledge, this is the first report of a VHH intrabody against HBcAg. Despite their preliminary character, our data seem to indicate that HBcAg-specific VHH intrabodies have an effect on the viral life cycle in HBV-transfected hepatocytes. The molecular mechanism of this VHH-mediated effect on HBV needs to be elucidated in future experiments. The inability to detect HBcAg in lysates of HBV-transfected cells that were cotransfected with a nuclear VHH intrabody needs to be examined in more detail. It may be worthwhile to examine the effects of a combined transfection with a nuclear and a cytoplasmic VHH construct to see if this results in a stronger inhibition of HBV replication and particle production. Study of these VHH intrabodies *in vivo* will be of crucial importance to determine the antiviral capacity. As previously demonstrated with the S-specific VHHs, the antiviral effect observed in the *in vivo* model was much more convincing than that obtained in the *in vitro* cellular model. A combined targeting of HBsAg as well as HBcAg with their respective VHH intrabodies may also result in a more pronounced antiviral effect.

METHODS

Construction of the VHH phage display library and selection of HBcAg-specific VHHs. This protocol was carried out as described in the paper by Serruys *et al.* (2009).

VHH-binding ELISA. First, monomeric VHH molecules were produced and purified, according to the protocol described by Serruys *et al.* (2009). Maxisorp plates (Nunc) were coated with 1 μg HBcAg ml^{-1} (derived from HBV subtype *ayw* from Biodesign or HBV subtype *adw* from GlaxoSmithKline) or 1 μg HBeAg ml^{-1} (Diasorin). The plates were blocked with PBS/1 % BSA. After three washes with PBS/0.1 % Tween 20, VHHs were added at concentrations indicated on the figures. Afterwards, mouse anti-*myc* was added (Roche), followed by goat anti-mouse–horseradish peroxidase (HRP) conjugate (Sigma).

Also, a twofold serial dilution of the mAb mouse anti-core (Biodesign) was added to the coated plate as a positive control, followed by incubation with anti-mouse–HRP conjugate. HRP activity was determined with tetramethylbenzidine (TMB) substrate (Sigma). After addition of 0.5 M H_2SO_4, the OD was read at 450 nm.

Cloning of the VHH coding sequence in the eukaryotic pShooter vectors pCMV/*myc*/cyto and pCMV/*myc*/nuc. VHH sequences were amplified using one of the forward primers (FW) and the reverse primer RV. Since C2, C4 and C6 had an internal *Nco*I site, this extra restriction site had to be removed prior to further construction. For this, an extra amplification step was performed to amplify the sequences upstream and downstream of this extra *Nco*I site separately using the corresponding FW + RV_{intern} primer and the corresponding FW_{intern} + RV primer, respectively. Both amplification products were used for a final PCR with the FW and RV primers, resulting in an amplified VHH sequence without the internal restriction site. PCR primers are listed in Supplementary Table S1. Next, PCR fragments were digested with *Not*I and *Nco*I and ligated into the nuclear plasmid pCMV/*myc*/nuc or the cytoplasmic plasmid pCMV/*myc*/cyto (pShooter, Invitrogen). Finally, *E. coli* TOP10 cells (Invitrogen) were transformed with this ligation product.

Cells and transfections. HepG2 cells were grown in cRPMI medium (RPMI medium, 10 % fetal calf serum, 100 U penicillin ml^{-1}, 100 μg streptomycin ml^{-1}, 1 mM sodium pyruvate, 2 mM L-glutamine) at 37 °C in a humidified 5 % CO_2 atmosphere. Twenty-four hours before transfection, cells were transferred to cRPMI medium with 0.1 mM dithiothreitol (DTT) and 10 mM glucose. Transfection of 4×10^6 cells with 20 μg plasmid was performed by electroporation at 250 V and 975 μF in 300 μl cRPMI (without fetal calf serum) with 0.1 mM DTT and 10 mM glucose. For lysate purposes, electroporated cells were resuspended in 6 ml cRPMI and kept in a cell culture flask for 3 days. For immunostaining purposes, the electroporated cells were resuspended in 9 ml cRPMI and 3 ml of this suspension was added to coverslips in a six-well plate. Five–six hours after transfection, the supernatant was replaced completely by fresh medium. Supernatant (1 ml) was collected 3 days post-electroporation. HepG2 cells were harvested by EDTA/trypsin treatment. After two washes with PBS, the cells were lysed by five freeze/thaw cycles in 200 μl PBS/1 × complete protease inhibitor cocktail (Boehringer Mannheim). After centrifugation, the protein concentration of the cleared cell lysate was measured (protein assay dye reagent from Bio-Rad).

Sandwich-VHH-binding ELISA Maxisorp plates were coated with 10 μg rabbit-anti-HBcAg ml^{-1} (Dako) for 2 h. The plates were blocked with PBS/1 % BSA. Forty-five micrograms total lysate or 50 ng purified HBcAg ml^{-1} was added and incubated overnight at 4 °C. After five washes with PBS/0.05 % Tween 20, 1 μg VHH ml^{-1} was added and incubated for 1 h at room temperature. VHH detection was performed by incubation with mouse anti-myc– and goat anti-mouse–HRP. Also, mouse anti-HBcAg was added as a positive control for HBcAg detection, followed by goat anti-mouse–HRP incubation. HRP activity was determined with TMB substrate and stopped by adding 0.5 M H_2SO_4. The OD was read at 450 nm.

HBcAg detection ELISA A Maxisorp plate was coated with 10 μg rabbit anti-HBcAg ml^{-1} (Dako) and coated with PBS/1 % BSA. Lysates were added at the concentrations indicated. After three washes with PBS/0.05 % Tween 20, detection of bound HBcAg was carried out with mouse anti-HBcAg– and goat anti-mouse–HRP.

Analysis of HBV parameters in transfected cells. HBsAg and HBeAg levels were determined in cell culture supernatant and lysates with the HBsAg (V2) AxSYM test and HBeAg 2.0 AxSYM test (Abbott), respectively. The detection limit for HBsAg is 2 signal-to-noise (S/N) while for HBeAg the cutoff value is 1 signal-to-cutoff (S/Co).

Immunostaining of electroporated HepG2 cells. Cells grown on coverslips were washed with PBS, fixed with 4 % paraformaldehyde, permeabilized with 0.1 % Triton X-100 and blocked in PBS/10 % goat serum for 30 min. VHHs were detected using mouse anti-*myc* and goat anti-mouse AlexaFluor 546 (Molecular Probes). HBcAg was detected with rabbit anti-HBcAg and goat anti-Rabbit 488 (Molecular Probes). Nuclei were stained with DAPI (Molecular Probes). Coverslips were mounted in Vectashield mounting medium (Vector) and examined with a confocal laser scanning microscope (Carl Zeiss Microscopes).

ACKNOWLEDGEMENTS

This research was supported by the Institute for the Promotion of Innovation through Science and Technology in Flanders (IWT-Vlaanderen). We thank Frank Chisari for providing the pSP65ayw1.3 plasmid and Hamida Hammad for her assistance with the confocal microscopy.

REFERENCES

Bruss, V. (2004). Envelopment of the hepatitis B virus nucleocapsid. *Virus Res* **106**, 199–209.

Bruss, V. (2007). Hepatitis B virus morphogenesis. *World J Gastroenterol* **13**, 65–73.

Butz, K., Denk, C., Fitscher, B., Crnkovic-Mertens, I., Ullmann, A., Schröder, C. H. & Hoppe-Seyler, F. (2001). Peptide aptamers targeting the hepatitis B virus core protein: a new class of molecules with antiviral activity. *Oncogene* **20**, 6579–6586.

Deres, K., Schröder, C. H., Paessens, A., Goldmann, S., Hacker, H. J., Weber, O., Krämer, T., Niewöhner, U., Pleiss, U. & other authors (2003). Inhibition of hepatitis B virus replication by drug-induced depletion of nucleocapsids. *Science* **299**, 893–896.

Feld, J., Lee, J. Y. & Locarnini, S. (2003). New targets and possible new therapeutic approaches in the chemotherapy of chronic hepatitis B. *Hepatology* **38**, 545–553.

Feng, Y., Kong, Y. Y., Wang, Y. & Qi, G. R. (2001). Intracellular inhibition of the replication of hepatitis B virus by hammerhead ribozymes. *J Gastroenterol Hepatol* **16**, 1125–1130.

Gordien, E., Rosmorduc, O., Peltekian, C., Garreau, F., Brechot, C. & Kremsdorf, D. (2001). Inhibition of hepatitis B virus replication by the interferon-inducible MxA protein. *J Virol* **75**, 2684–2691.

Hilleman, M. R. (2003). Critical overview and outlook: pathogenesis, prevention, and treatment of hepatitis and hepatocarcinoma caused by hepatitis B virus. *Vaccine* **21**, 4626–4649.

Ji, W. & Si, C. W. (1997). Inhibition of hepatitis B virus by retroviral vectors expressing antisense RNA. *J Viral Hepat* **4**, 167–173.

Kann, M., Schmitz, A. & Rabe, B. (2007). Intracellular transport of hepatitis B virus. *World J Gastroenterol* **13**, 39–47.

Kim, T. H., Cho, E. Y., Oh, H. J., Choi, C. S., Kim, J. W., Moon, H. B. & Kim, H. C. (2006). The degrees of hepatocyte cytoplasmic expression of hepatitis B core antigen correlate with histologic activity of liver disease in the young patients with chronic hepatitis B infection. *J Korean Med Sci* **21**, 279–283.

Lavanchy, D. (2004). Hepatitis B virus epidemiology, disease burden, treatment, and current and emerging prevention and control measures. *J Viral Hepat* **11**, 97–107.

Rabe, B., Vlachou, A., Pante, N., Helenius, A. & Kann, M. (2003). Nuclear import of hepatitis B virus capsids and release of the viral genome. *Proc Natl Acad Sci U S A* **100**, 9849–9854.

Rosmorduc, O., Sirma, H., Soussan, P., Gordien, E., Lebon, P., Horisberger, M., Brechot, C. & Kremsdorf, D. (1999). Inhibition of interferon-inducible MxA protein expression by hepatitis B virus capsid protein. *J Gen Virol* **80**, 1253–1262.

Seeger, C., Zoulim, F. & Mason, W. S. (2007). Hepadnaviruses. In *Fields Virology*, 5th edn, pp. 2977–3029. Edited by D. M. Knipe & P. M. Howley. Philadelphia, PA: Lippincott Williams and Wilkins.

Serinoz, E., Varli, M., Erden, E., Cinar, K., Kansu, A., Uzunalimoglu, O., Yurdaydin, C. & Bozkaya, H. (2003). Nuclear localization of hepatitis B core antigen and its relations to liver injury, hepatocyte proliferation, and viral load. *J Clin Gastroenterol* **36**, 269–272.

Serruys, B., Van Houtte, F., Verbrugghe, P., Leroux-Roels, G. & Vanlandschoot, P. (2009). Llama-derived single-domain intrabodies inhibit secretion of hepatitis B virions in mice. *Hepatology* **49**, 39–49.

Tuttleman, J. S., Pourcel, C. & Summers, J. (1986). Formation of the pool of covalently closed circular viral DNA in hepadnavirus-infected cells. *Cell* **47**, 451–460.

Xu, R., Cai, K., Zheng, D., Ma, H., Xu, S. & Fan, S. T. (2003). Molecular therapeutics of HBV. *Curr Gene Ther* **3**, 341–355.

Yamamoto, M., Hayashi, N., Takehara, T., Ueda, K., Mita, E., Tatsumi, T., Sasaki, Y., Kasahara, A. & Hori, M. (1999). Intracellular single-chain antibody against hepatitis B virus core protein inhibits the replication of hepatitis B virus in cultured cells. *Hepatology* **30**, 300–307.

Ying, C., De Clercq, E. & Neyts, J. (2003). Selective inhibition of hepatitis B virus replication by RNA interference. *Biochem Biophys Res Commun* **309**, 482–484.